



Original Article

The Influence of the Scalar and Vector Anomalous Couplings on the Z-production at ILC in the Randall - Sundrum Model

Bui Thi Ha Giang*

Hanoi National University of Education, 136 Xuan Thuy, Cau Giay, Hanoi, Vietnam

Received 7 April 2023

Revised 4 May 2023; Accepted 4 May 2023

Abstract: An attempt is made to present the effect of the scalar and vector anomalous couplings on e^-e^+ scattering process with polarized initial beams in the Randall-Sundrum model. We have studied the contribution of radion, Higgs and gauge bosons on the Z-production cross-section at International Linear Colliders (ILC). The cross-section depends strongly on the polarization of e^- , e^+ initial beams, the center of mass energy \sqrt{s} and model interaction parameters. The obtained results indicate that with the vector anomalous couplings included Z boson and photon, the cross-sections for the Z production are much larger than that with the scalar couplings included radion and Higgs under the same conditions.

Keywords: Z production, cross-section, scalar anomalous couplings, vector anomalous couplings.

1. Introduction

The existence of some theoretical drawbacks motivates the new models beyond the Standard model (SM). The Randall-Sundrum (RS) model is one of the most attractive extended SM models. The RS is a theoretical framework to explain the hierarchy problem, which refers to the large discrepancy between the weak scale and the Planck scale. One of the interesting consequences of the RS model is the existence of an additional scalar called the radion (ϕ) [1]. Radion and Higgs boson have the same quantum numbers. Radion can interact with matter. Its production and decay can lead to interesting experimental signatures, such as missing energy in collider experiments. Therefore, radion is a potential candidate for

* Corresponding author.

E-mail address: giangbth@hnue.edu.vn

<https://doi.org/10.25073/2588-1124/vnumap.4842>

dark matter. The radion couplings to $\gamma\gamma$, gg and $Z\gamma$ are dominated in the region $\xi \in [0, 0.3]$ [2]. It is of particular interest to analyse the radion couplings in conformal limit $\xi = 1/6$.

The trilinear gauge boson couplings have been important in testing the electroweak interactions [3]. Diboson production, in particular ZZ and W^+W^- , are also extensively used in Higgs boson measurements [4]. Moreover, the anomalous vertices include ZZZ , γZZ , $\gamma\gamma Z$ interactions, which are not present at tree level in SM, have been widely discussed in the different colliders: e^-e^+ collider, γe^- collider, hadron collider [3, 5-11]. In experiments, the cross-section for Z production in $p\bar{p}$ collisions has been measured by both the ATLAS and CMS collaboration [12-16]. Because of clean electron and positron sources at ILC, Z boson produced at the high energy collisions could give the possible measurement. Any possible new physics in the Z boson production collision is expected to change the cross-section.

In this work, we have only considered the $e^-e^+ \rightarrow ZZ \rightarrow l^+l^-q\bar{q}$, $e^+e^- \rightarrow \gamma Z \rightarrow \gamma l^+l^-$ processes in s-channel, included the vertices of Z boson as ZZZ , γZZ , $\gamma\gamma Z$, ϕZZ , hZZ , γZh , $\gamma Z\phi$. The layout of this work is as follows. In Section II, we review the scalar and vector anomalous couplings. The influence of the scalar and vector anomalous couplings on the Z production at ILC is presented in Section III. Finally, we summarize our results and draw conclusions in Section IV.

2. A Review of the Scalar and Vector Anomalous Couplings

In Randall – Sundrum model, due to the same quantum numbers, radion and Higgs boson can be mixed. The mixing parameter ξ mixes the h_0 and ϕ_0 fields into the mass eigenstates h and ϕ as given by

$$\begin{pmatrix} h_0 \\ \phi_0 \end{pmatrix} = \begin{pmatrix} 1 & -6\xi\gamma/Z \\ 0 & 1/Z \end{pmatrix} \begin{pmatrix} \cos\theta & \sin\theta \\ -\sin\theta & \cos\theta \end{pmatrix} \begin{pmatrix} h \\ \phi \end{pmatrix} = \begin{pmatrix} d & c \\ b & a \end{pmatrix} \begin{pmatrix} h \\ \phi \end{pmatrix}, \quad (1)$$

where

$$\gamma \equiv \nu_0 / \Lambda_\phi, Z^2 \equiv 1 - 6\xi\gamma^2(1 + 6\xi) = \beta - 36\xi^2\gamma^2, \beta = 1 - 6\xi\gamma^2, \quad (2)$$

$$a = \frac{\cos\theta}{Z}, b = -\frac{\sin\theta}{Z}, c = \sin\theta - \frac{6\xi\gamma}{Z}\cos\theta, d = \cos\theta + \frac{6\xi\gamma}{Z}\sin\theta. \quad (3)$$

The mixing angle θ is defined by

$$\tan 2\theta = 12\gamma\xi Z \frac{m_{h_0}^2}{m_{h_0}^2(Z^2 - 36\xi^2\gamma^2) - m_{\phi_0}^2}. \quad (4)$$

The new physical fields h and ϕ are Higgs-dominated state and radion, respectively

$$m_{h,\phi}^2 = \frac{1}{2Z^2} \left[m_{\phi_0}^2 + \beta m_{h_0}^2 \pm \sqrt{(m_{\phi_0}^2 + \beta m_{h_0}^2)^2 - 4Z^2 m_{\phi_0}^2 m_{h_0}^2} \right]. \quad (5)$$

When $\xi \neq 0$, there are four independent parameters that must be specified to fix the state mixing parameters a, b, c, d of Eq. (3) defining the mass eigenstates $\Lambda_\phi, m_h, m_\phi, \xi$.

Feynman rules for the couplings are showed as follows [2]

$$g_{eeh} = i\bar{g}_{eeh} = -i \frac{gm_e}{2m_W} (d + \gamma b), \tag{6}$$

$$g_{ee\phi} = i\bar{g}_{ee\phi} = -i \frac{gm_e}{2m_W} (c + \gamma a), \tag{7}$$

$$g_{hZZ}^{\mu\nu} = i\bar{g}_{hZ} \left[\eta^{\mu\nu} - 2g_h^Z (k_1 k_2 \eta^{\mu\nu} - k_1^\nu k_2^\mu) \right], \tag{8}$$

$$g_{\phi ZZ}^{\mu\nu} = i\bar{g}_{\phi Z} \left[\eta^{\mu\nu} - 2g_\phi^Z (k_1 k_2 \eta^{\mu\nu} - k_1^\nu k_2^\mu) \right]. \tag{9}$$

$$\begin{aligned} g_{\gamma Zh}^{\mu\nu} &= iC_{\gamma Zh} \left[k_1 k_2 \eta^{\mu\nu} - k_1^\nu k_2^\mu \right] \\ &= i \frac{\alpha}{2\pi\nu_0} \left[2g_h^r \left(\frac{b_2}{\tan\theta_W} - b_Y \tan\theta_W \right) - g_h (A_F + A_W) \right] \left[k_1 k_2 \eta^{\mu\nu} - k_1^\nu k_2^\mu \right], \end{aligned} \tag{10}$$

$$\begin{aligned} g_{\gamma Z\phi}^{\mu\nu} &= iC_{\gamma Z\phi} \left[k_1 k_2 \eta^{\mu\nu} - k_1^\nu k_2^\mu \right] \\ &= i \frac{\alpha}{2\pi\nu_0} \left[2g_\phi^r \left(\frac{b_2}{\tan\theta_W} - b_Y \tan\theta_W \right) - g_\phi (A_F + A_W) \right] \left[k_1 k_2 \eta^{\mu\nu} - k_1^\nu k_2^\mu \right]. \end{aligned} \tag{11}$$

Here, $\bar{g}_{eZ}, \bar{g}_{hZ}, \bar{g}_{\phi Z}$ can be found in Ref. [2, 17-18], the triangle loop functions A_F, A_W are given in Ref. [19].

The triple gauge boson couplings are given by [10]

$$\begin{aligned} \Gamma_{\gamma ZZ}^{\mu\nu\sigma}(q, k_1, k_2) &= \frac{g_e}{M_Z^2} \left[f_4^\gamma \left((k_2^\nu g^{\mu\sigma} + k_1^\sigma g^{\mu\nu}) q^2 - q^\mu (k_1^\sigma q^\nu + k_2^\nu q^\sigma) \right) + f_5^\gamma \left(q^\mu q_\beta \varepsilon^{\nu\sigma\alpha\beta} + q^2 \varepsilon^{\mu\nu\sigma\alpha} \right) (k_1 - k_2)_\alpha \right. \\ &\quad + h_1^Z \left(k_2^\mu q^\nu k_2^\sigma + k_1^\mu k_1^\nu q^\sigma + (k_1^2 - k_2^2) (q^\nu g^{\mu\sigma} - q^\sigma g^{\mu\nu}) - k_2^\sigma g^{\mu\nu} q \cdot k_2 - k_1^\nu g^{\mu\sigma} q \cdot k_1 \right) \\ &\quad \left. - h_3^Z \left(k_1^\nu k_{1\beta} \varepsilon^{\mu\sigma\alpha\beta} + k_{2\beta} k_2^\sigma \varepsilon^{\mu\nu\alpha\beta} + (k_2^2 - k_1^2) \varepsilon^{\mu\nu\sigma\alpha} \right) q_\alpha \right] \end{aligned} \tag{12}$$

$$\begin{aligned} \Gamma_{ZZZ}^{\mu\nu\sigma}(q, k_1, k_2) &= \frac{g_e}{M_Z^2} \left[f_4^Z \left(-q^\mu q^\nu k_1^\sigma - k_2^\mu q^\nu k_2^\sigma - k_2^\mu k_1^\nu k_1^\sigma - k_1^\mu k_2^\nu k_2^\sigma - (q^\mu k_2^\nu + k_1^\mu k_1^\nu) q^\sigma + g^{\mu\nu} (q^2 k_1^\sigma + k_1^2 q^\sigma) \right) \right. \\ &\quad + g^{\mu\sigma} (q^2 k_2^\nu + k_2^2 q^\nu) + g^{\nu\sigma} (k_2^2 k_1^\mu + k_1^2 k_2^\mu) - f_5^Z \left(\varepsilon^{\mu\nu\alpha\beta} (k_1 - q)_\alpha k_{2\beta} k_2^\sigma + \varepsilon^{\mu\nu\sigma\alpha} \left((k_1^2 - k_2^2) q_\alpha \right) \right. \\ &\quad \left. + (k_2^2 - q^2) k_{1\alpha} + (q^2 - k_1^2) k_{2\alpha} \right) + k_{1\beta} k_1^\nu (k_2 - q)_\alpha \varepsilon^{\mu\sigma\alpha\beta} + q_\beta q^\mu (k_2 - k_1)_\alpha \varepsilon^{\nu\sigma\alpha\beta} \left. \right] \end{aligned} \tag{13}$$

$$\begin{aligned} \Gamma_{\gamma\gamma Z}^{\mu\nu\sigma}(q, k_1, k_2) &= \frac{g_e}{M_Z^2} \left[h_1^\gamma \left(q^\mu q^\nu k_1^\sigma + q^\sigma k_1^\mu k_1^\nu - g^{\mu\nu} (q^2 k_1^\sigma + k_1^2 q^\sigma) + g^{\mu\sigma} (k_1^2 q^\nu - q \cdot k_1 k_1^\nu) \right) \right. \\ &\quad \left. + g^{\nu\sigma} (q^2 k_1^\mu - q \cdot k_1 q^\mu) - h_3^\gamma \left(k_{1\beta} k_1^\nu q_\alpha \varepsilon^{\mu\sigma\alpha\beta} + q^\mu k_{1\alpha} q_\beta \varepsilon^{\nu\sigma\alpha\beta} + (q^2 k_{1\alpha} - k_1^2 q_\alpha) \varepsilon^{\mu\nu\sigma\alpha} \right) \right]. \end{aligned} \tag{14}$$

3. The Influence of the New Anomalous Couplings on the Z Production at ILC

Vector boson pair production is interesting in itself as a test of the electroweak force and the presence of new physics [20]. In this work, we will evaluate the significance of the new couplings on the

Z-production, including the $e^-e^+ \rightarrow ZZ \rightarrow l^+l^-q\bar{q}$ and $e^+e^- \rightarrow \gamma Z \rightarrow \gamma l^+l^-$ processes only in s-channel with the polarized initial beams at ILC. An e^-e^+ collider is uniquely capable of operation at series of energies near the threshold of a new physics process. This is an extremely powerful tool for precision measurements of particle masses and unambiguous particle spin determinations [21].

3.1. The $e^-e^+ \rightarrow ZZ \rightarrow l^+l^-q\bar{q}$ Collision

We consider the collision process in which the initial state contains electron and positron.

$$e^-(p_1) + e^+(p_2) \rightarrow Z(k_1) + Z(k_2). \tag{15}$$

Here, p_i, k_i ($i = 1, 2$) stand for the momentums. There is Feynman diagram contributing to reaction (15), representing the s-channel exchange depicted in Fig. 1.

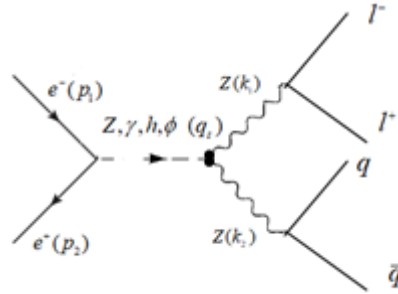


Figure 1. Feynman diagrams for $e^-e^+ \rightarrow ZZ \rightarrow l^+l^-q\bar{q}$ collision, representing the s-channel.

The transition amplitude representing the s-channel is given by

$$M_s = M_Z + M_\gamma + M_h + M_\phi, \tag{16}$$

here

$$M_Z = \frac{-\bar{g}_{eZ}}{q_s^2 - m_Z^2} \epsilon_\mu^*(k_1) \Gamma_{ZZ}^{\sigma\mu\nu}(q_s, k_1, k_2) \epsilon_\nu^*(k_2) \left(\eta_{\sigma\beta} - \frac{q_{s\sigma} q_{s\beta}}{m_Z^2} \right) \bar{v}(p_2) \gamma^\beta (v_e - a_e \gamma^5) u(p_1), \tag{17}$$

$$M_\gamma = \frac{-e}{q_s^2} \epsilon_\mu^*(k_1) \Gamma_{\gamma ZZ}^{\sigma\mu\nu}(q_s, k_1, k_2) \epsilon_\nu^*(k_2) \eta_{\sigma\beta} \bar{v}(p_2) \gamma^\beta u(p_1), \tag{18}$$

$$M_h = \frac{\bar{g}_{eh} \bar{g}_{hZ}}{q_s^2 - m_h^2} \epsilon_\mu^*(k_1) \left[\eta^{\mu\nu} - 2g_h^Z (k_1 k_2 \eta^{\mu\nu} - k_1^\nu k_2^\mu) \right] \epsilon_\nu^*(k_2) \bar{v}(p_2) u(p_1), \tag{19}$$

$$M_\phi = \frac{\bar{g}_{e\phi} \bar{g}_{\phi Z}}{q_s^2 - m_\phi^2} \epsilon_\mu^*(k_1) \left[\eta^{\mu\nu} - 2g_\phi^Z (k_1 k_2 \eta^{\mu\nu} - k_1^\nu k_2^\mu) \right] \epsilon_\nu^*(k_2) \bar{v}(p_2) u(p_1). \tag{20}$$

The cross-section for the whole process can be calculated as follow [10]

$$\sigma = \sigma(e^-e^+ \rightarrow ZZ) \times 2Br(Z \rightarrow l^+l^-) Br(Z \rightarrow q\bar{q}), \tag{21}$$

where

$$\frac{d\sigma(e^-e^+ \rightarrow ZZ)}{d(\cos\psi)} = \frac{1}{32\pi s} \frac{|\vec{k}_1|}{|\vec{p}_1|} |M_{fi}|^2 \tag{22}$$

is the expression of the differential cross-section [22]. $\psi = (\vec{p}_1, \vec{k}_1)$ is the scattering angle.

For numerical evaluation, we choose ILC running at a center-of-mass energy of 500 GeV. The vacuum expectation value (VEV) of the radion field was set as $A_\phi = 5$ TeV. The radion mass was set as $m_\phi = 10$ GeV. The Higgs mass was set as $m_h = 125$ GeV. The maximum value of anomalous couplings in the tightest limits with the corresponding observable were set as $f_4^\gamma = 2.4 \times 10^{-3}$, $f_4^Z = 4.2 \times 10^{-3}$, $f_5^\gamma = 2.7 \times 10^{-3}$, $f_5^Z = 8.8 \times 10^{-3}$, $h_1^\gamma = 3.6 \times 10^{-3}$, $h_3^\gamma = 1.3 \times 10^{-3}$, $h_1^Z = 2.9 \times 10^{-3}$, $h_3^Z = 2.8 \times 10^{-3}$ [10].

We give estimates for the cross-sections as follows:

i) In Fig. 2, the cross-sections are plotted as the function of P_{e^-}, P_{e^+} , which are the polarization coefficients of e^-, e^+ beams, respectively. The figure indicates that the cross-section in case of vector propagators (Z boson and photon) achieves the maximum value when $P_{e^-} = P_{e^+} = \pm 1$ and the minimum value when $P_{e^-} = 1, P_{e^+} = -1$ or $P_{e^-} = -1, P_{e^+} = 1$. This result reverses the consequence in case of scalar propagators (radion and Higgs);

ii) In the case of $P_{e^-} = 0.8, P_{e^+} = -0.3$ [23, 24], the $f_i^{\gamma/Z}$ chosen as Fig. 2, the cross-sections are measured in the case of the different collision energy \sqrt{s} in Fig. 3. The cross-sections increase when the collision energy increases. The cross-section increases fast in case of vector anomalous couplings while the cross-section increases gradually in case of scalar anomalous couplings;

iii) Some numerical values for cross-section in $e^-e^+ \rightarrow ZZ \rightarrow l^+l^-q\bar{q}$ are shown in Table 1. With the gauge boson contribution, the cross-section is much larger than that with radion, Higgs contribution.

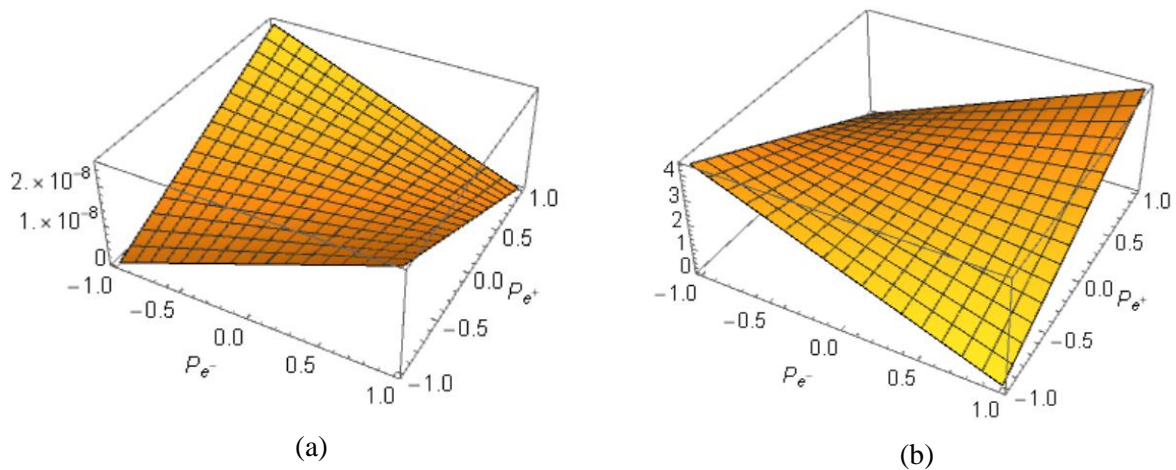


Figure 2. The cross-section as a function of the polarization coefficients (P_{e^-}, P_{e^+}) in $e^-e^+ \rightarrow ZZ \rightarrow l^+l^-q\bar{q}$ collision in case of (a) scalar anomalous couplings, (b) vector anomalous couplings.

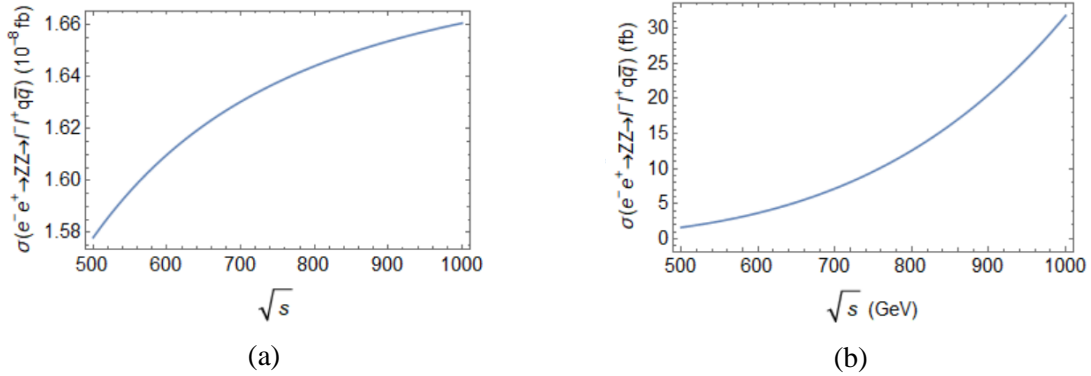


Figure 3. The cross-section as a function of the collision energy in $e^-e^+ \rightarrow ZZ \rightarrow l^+l^-q\bar{q}$ collision in case of (a) scalar anomalous couplings, (b) vector anomalous couplings.

Table 1. Typical values for the cross-section in the $e^-e^+ \rightarrow ZZ \rightarrow l^+l^-q\bar{q}$ collision at the ILC in the case of $P_{e^-} = 0.8, P_{e^+} = -0.3$

\sqrt{s} (GeV)	500	600	700	800	900	1000
$\sigma_{Z,\gamma}(e^-e^+ \rightarrow ZZ \rightarrow l^+l^-q\bar{q})$ (fb)	1.665	3.719	7.196	12.620	20.596	31.809
$\sigma_{\phi,h}(e^-e^+ \rightarrow ZZ \rightarrow l^+l^-q\bar{q})$ (10^{-8} fb)	1.578	1.610	1.630	1.644	1.653	1.660

3.2. The $e^+e^- \rightarrow \gamma Z \rightarrow \gamma l^+l^-$ Collision

We consider the collision process in which the initial state contains electron and positron.

$$e^-(p_1) + e^+(p_2) \rightarrow \gamma(k_1) + Z(k_2). \tag{23}$$

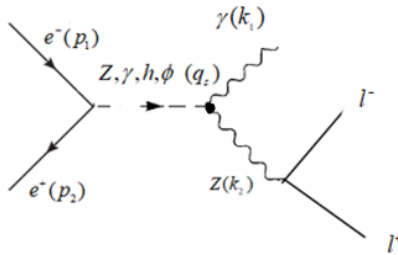


Figure 4. Feynman diagrams for $e^+e^- \rightarrow \gamma Z \rightarrow \gamma l^+l^-$ collision in s-channel.

There is Feynman diagram contributing to reaction (23), representing the s-channel exchange depicted in Fig. 4. The transition amplitude representing the s-channel is given by

$$M_s = M_Z + M_\gamma + M_h + M_\phi, \tag{24}$$

here

$$M_Z = \frac{-\bar{g}_{eZ}}{q_s^2 - m_Z^2} \varepsilon_\mu^*(k_1) \Gamma_{\gamma ZZ}^{\sigma\mu\nu}(q_s, k_1, k_2) \varepsilon_\nu^*(k_2) \left(\eta_{\sigma\beta} - \frac{q_{s\sigma} q_{s\beta}}{m_Z^2} \right) \bar{v}(p_2) \gamma^\beta (v_e - a_e \gamma^5) u(p_1), \tag{25}$$

$$M_\gamma = \frac{-e}{q_s^2} \varepsilon_\mu^*(k_1) \Gamma_{\gamma\gamma Z}^{\sigma\mu\nu}(q_s, k_1, k_2) \varepsilon_\nu^*(k_2) \eta_{\sigma\beta} \bar{v}(p_2) \gamma^\beta u(p_1), \tag{26}$$

$$M_h = \frac{\bar{g}_{e\phi} C_{\gamma Zh}}{q_s^2 - m_h^2} \varepsilon_\mu^*(k_1) [k_1 k_2 \eta^{\mu\nu} - k_1^\nu k_2^\mu] \varepsilon_\nu^*(k_2) \bar{v}(p_2) u(p_1), \tag{27}$$

$$M_\phi = \frac{\bar{g}_{e\phi} C_{\gamma Z\phi}}{q_s^2 - m_\phi^2} \varepsilon_\mu^*(k_1) [k_1 k_2 \eta^{\mu\nu} - k_1^\nu k_2^\mu] \varepsilon_\nu^*(k_2) \bar{v}(p_2) u(p_1), \tag{28}$$

The cross-section for the whole process $e^+e^- \rightarrow \gamma Z \rightarrow \gamma l^+ l^-$ can be calculated as follows

$$\sigma = \sigma(e^+e^- \rightarrow \gamma Z) \times Br(Z \rightarrow l^+ l^-). \tag{29}$$

We estimate the total cross-section for $\gamma l^+ l^-$ production as follows:

i) The parameters $f_4^V, f_5^V, h_1^V, h_3^V$ ($V = \gamma, Z$) are taken as Fig. 2. The Fig. 5 indicates that the cross-section in case of vector propagators (Z boson and photon) achieves the maximum value when $P_{e^-} = P_{e^+} = \pm 1$ and the minimum value when $P_{e^-} = 1, P_{e^+} = -1$ or $P_{e^-} = -1, P_{e^+} = 1$. This result reverses the consequence in case of scalar propagators (radion and Higgs);

ii) With the parameters $f_4^V, f_5^V, h_1^V, h_3^V$ ($V = \gamma, Z$) as Fig. 2, $P_{e^-} = 0.8, P_{e^+} = -0.3$, the total cross-sections are measured in the case of the different collision energy \sqrt{s} in Fig. 6. The cross-sections in case of scalar propagators decrease gradually when the collision energy increases while the cross-section increases fast in case of vector anomalous couplings;

iii) Some numerical values for cross-section in $e^+e^- \rightarrow \gamma Z \rightarrow \gamma l^+ l^-$ are shown in Table 2. With the gauge boson contribution, the cross-section is much larger than that with radion, Higgs contribution;

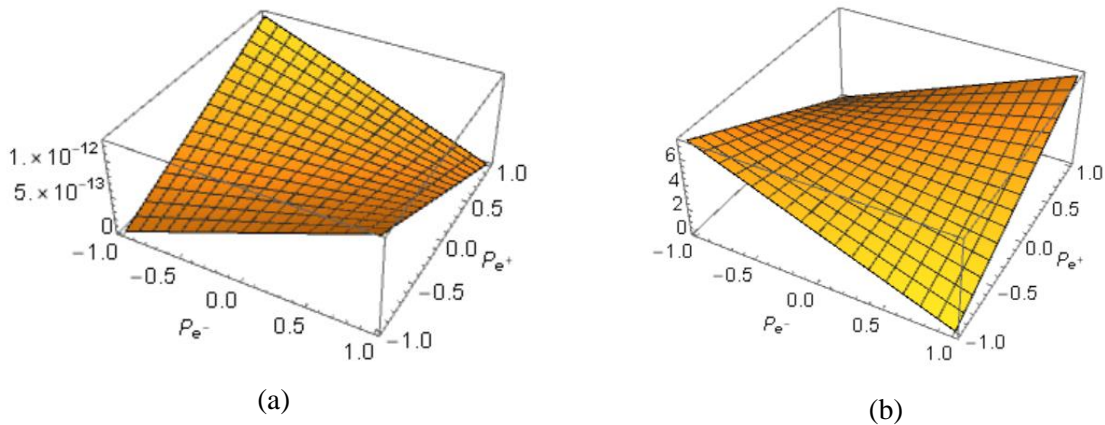


Figure 5. The cross-section as a function of the polarization coefficients (P_{e^-}, P_{e^+}) in $e^+e^- \rightarrow \gamma Z \rightarrow \gamma l^+ l^-$ collision in case of (a) scalar anomalous couplings, (b) vector anomalous couplings.

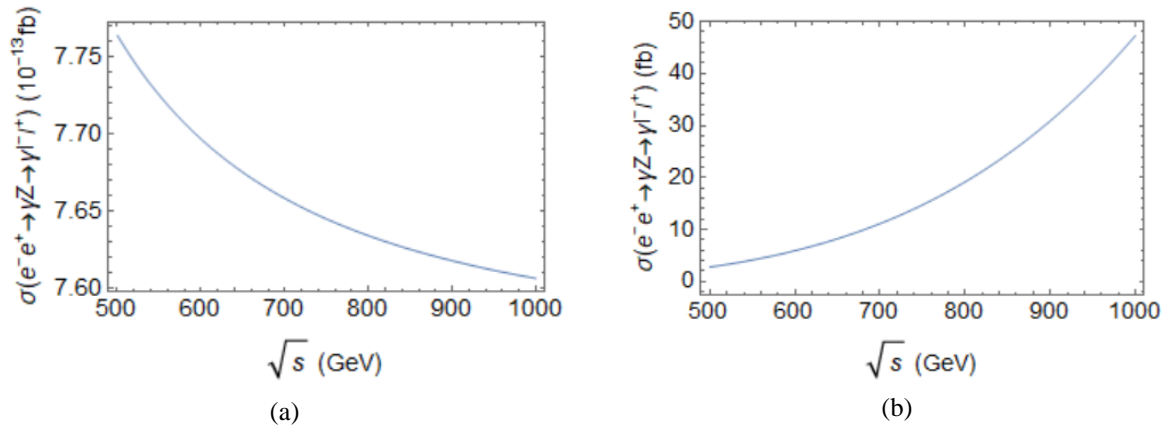


Figure 6. The cross-section for the whole process $e^+e^- \rightarrow \gamma Z \rightarrow \gamma l^+l^-$ collision as a function of the collision energy \sqrt{s} in case of (a) scalar anomalous couplings, (b) vector anomalous couplings.

Table 2. Typical values for the cross-section in the $e^+e^- \rightarrow \gamma Z \rightarrow \gamma l^+l^-$ collision at the ILC in the case of $P_{e^-} = 0.8, P_{e^+} = -0.3$.

$\sqrt{s} (GeV)$	500	600	700	800	900	1000
$\sigma_{z,\gamma}(e^+e^- \rightarrow \gamma Z \rightarrow \gamma l^+l^-)$ (fb)	2.800	5.937	11.145	19.176	30.894	47.282
$\sigma_{\phi,h}(e^+e^- \rightarrow \gamma Z \rightarrow \gamma l^+l^-)$ (10^{-13} fb)	7.763	7.696	7.658	7.634	7.618	7.606

4. Conclusion

In this work, we have studied the contribution of the new anomalous couplings on the ZZ, γZ production at ILC in the RS model. With the available value of parameters $f_4^V, f_5^V (V = \gamma, Z)$, the results indicate that with the vector anomalous couplings, the cross-sections for the Z production are enhanced and much larger than that in the scalar anomalous couplings under the same conditions. Although the influence is quite small, the scalar anomalous couplings which appear in high energy collisions are a key tool in the search for physics beyond the SM. In our future works, we are studying the scalar anomalous couplings in pp collisions at the Large Hadron Collider (LHC) to search the signal of new particles and interactions.

References

[1] L. Randall, R. Sundrum, A Large Mass Hierarchy from a Small Extra Dimension, Physical Review Letters, Vol. 83, Iss. 17, 1999, pp. 3370-3373, <https://doi.org/10.1103/PhysRevLett.83.3370>.
 [2] A. Ahmed, B. M. Dillon, B. Grzadkowski, J. F. Gunion, Y. Jiang, Implications of the Absence of High-mass Radion Signals, Physical Review D, Vol. 95, Iss. 9, 2017, 095019, <https://doi.org/10.1103/PhysRevD.95.095019>.
 [3] S. Atag, I. Sahin, ZZ γ and Z $\gamma\gamma$ Couplings in γe Collisions with Polarized Beams, Physical Review D, Vol. 68, Iss. 9, 2003, 093014, <https://doi.org/10.1103/PhysRevD.68.093014>.

- [4] S. Kallweit, M. Wiesemann, ZZ Production at the LHC: NNLO Predictions for $2\ell 2\nu$ and 4ℓ Signatures, *Physics Letters B*, Vol. 786, 2018, pp. 382-389, <https://doi.org/10.1016/j.physletb.2018.10.016>.
- [5] G. J. Gounaris, J. Layssac, F. M. Renard, Signatures of the Anomalous $Z\gamma$ and ZZ Production at the Lepton and Hadron Colliders, *Physical Review D*, Vol. 61, Iss. 7, 2000, 073013,
- [6] <https://doi.org/10.1103/PhysRevD.61.073013>.
- [7] U. Baur, D. L. Rainwater, Probing Neutral Gauge Boson Self Interactions in ZZ Production at Hadron Colliders, *Physical Review D*, Vol. 62, Iss. 11, 2000, 113011, <https://doi.org/10.1103/PhysRevD.62.113011>.
- [8] B. Ananthanarayan, S. D. Rindani, R. K. Singh, A. Bartl, Transverse Beam Polarization and CP-violating Triple Gauge Boson Couplings in $e^+e^- \rightarrow \gamma Z$, *Physics Letters B*, Vol. 593, 2004, pp. 95-104, <https://doi.org/10.1016/j.physletb.2004.04.067>.
- [9] B. Ananthanarayan, S. K. Garg, M. Patra, S. D. Rindani, Isolating CP-violating γZZ Coupling in $e^+e^- \rightarrow \gamma Z$ with Transverse Beam Polarizations, *Physical Review D*, Vol. 85, Iss. 3, 2012, pp. 034006, <https://doi.org/10.1103/PhysRevD.85.034006>.
- [10] B. Ananthanarayan, J. Lahiri, M. Patra, S. D. Rindani, New Physics in $e^+e^- \rightarrow \gamma Z$ at the ILC with Polarized beams: Explorations beyond Conventional Anomalous Triple Gauge Boson Couplings, *Journal of High Energy Physics*, Vol. 08, 2014, pp. 124, [https://doi.org/10.1007/JHEP08\(2014\)124](https://doi.org/10.1007/JHEP08(2014)124).
- [11] R. Rahaman, R. K. Singh, On Polarization Parameters of Spin-1 Particles and Anomalous Couplings in $e^+e^- \rightarrow ZZ / Z\gamma$, *The European Physical Journal C*, Vol. 76, 2016, pp. 539, <https://doi.org/10.1140/epjc/s10052-016-4374-4>.
- [12] F. Cascioli et al., ZZ Production at Hadron Colliders in NNLO QCD, *Physics Letters B*, Vol. 735, 2014, pp. 311-313, <https://doi.org/10.1016/j.physletb.2014.06.056>.
- [13] ATLAS collaboration, Measurement of the ZZ Production Cross Section in Proton-Proton Collisions at $\sqrt{s} = 8$ TeV using the $ZZ \rightarrow l^-l^+l^-l^+$ and $ZZ \rightarrow l^-l^+\nu\bar{\nu}$ Channels with the ATLAS Detector, *Journal of High Energy Physics*, Vol. 01, 2017, pp. 099, [https://doi.org/10.1007/JHEP01\(2017\)099](https://doi.org/10.1007/JHEP01(2017)099).
- [14] ATLAS Collaboration, Measurement of ZZ Production in pp Collisions at $\sqrt{s} = 7$ TeV and Limits on Anomalous ZZZ and ZZ γ Couplings with the ATLAS Detector, *Journal of High Energy Physics*, Vol. 03, 2013, pp. 128, [https://doi.org/10.1007/JHEP03\(2013\)128](https://doi.org/10.1007/JHEP03(2013)128).
- [15] CMS Collaboration, Measurement of the ZZ Production Cross Section and Search for Anomalous Couplings in $2l2l'$ Final States in pp Collisions at $\sqrt{s} = 7$ TeV, *Journal of High Energy Physics*, Vol. 01, 2013, pp. 063, [https://doi.org/10.1007/JHEP01\(2013\)063](https://doi.org/10.1007/JHEP01(2013)063).
- [16] ATLAS Collaboration, Measurement of the ZZ Production Cross Section in pp Collisions at $\sqrt{s} = 13$ TeV with the ATLAS Detector, *Physical Review Letters*, Vol. 116, Iss. 10, 2016, pp. 101801, <https://doi.org/10.1103/PhysRevLett.116.101801>.
- [17] ATLAS Collaboration, Measurements of Four-Lepton Production in pp Collisions at $\sqrt{s} = 8$ TeV with the ATLAS Detector, *Physics Letters B*, Vol. 753, 2016, pp. 552-572, <https://doi.org/10.1016/j.physletb.2015.12.048>.
- [18] D. Dominici, B. Grzadkowski, J. F. Gunion, and M. Toharia, The Scalar Sector of the Randall-Sundrum model, *Nuclear Physics B*, Vol. 671, 2003, pp. 243-292, <https://doi.org/10.1016/j.nuclphysb.2003.08.020>.
- [19] B. Grzadkowski, J. F. Gunion, and M. Toharia, Higgs-Radion Interpretation of the LHC Data?, *Physics Letters B*, Vol. 712, 2012, pp. 70-80, <https://doi.org/10.1016/j.physletb.2012.04.037>.
- [20] J. F. Gunion, H. E. Haber, G. L. Kane et al., *The Higgs Hunter's Guide*, CRC Press, 2000.
- [21] T. Melia, P. Nason, R. Rontsch, G. Zanderighi, W^+W^- , WZ and ZZ Production in the POWHEG BOX, *Journal of High Energy Physics*, Vol. 11, 2011, pp. 078, [https://doi.org/10.1007/JHEP11\(2011\)078](https://doi.org/10.1007/JHEP11(2011)078).
- [22] T. Kikuchi, N. Okada, M. Takeuchi, Unparticle Physics at the Photon Collider, *Physical Review D*, Vol. 77, Iss. 9, 2008, pp. 094012, <https://doi.org/10.1103/PhysRevD.77.094012>.
- [23] M. E. Peskin, D. V. Schroeder, *An Introduction to Quantum Field Theory*, CRC Press, 1995.
- [24] A. Vauth, J. List, Beam Polarization at the ILC: Physics Case and Realization, *International Journal of Modern Physics: Conference Series*, Vol. 40, 2016, pp. 1660003, <https://doi.org/10.1142/S201019451660003X>.
- [25] H. Abramowicz et al., Higgs Physics at the CLIC Electron-Positron Linear Collider, *The European Physical Journal C*, Vol. 77, 2017, pp. 475, <https://doi.org/10.1140/epjc/s10052-017-4968-5>.